Practical Insights for Microgrid Operation with Energy Management Capable Prosumers

Pedro Torres[1], Kauê N. de Souza[1], Alex Manito[1], Roberto Zilles[1], João T. Pinho[1,2]

[1] Institute of Energy and Environment – Universidade de São Paulo, São Paulo (Brazil)

[2] Grupo de Estudos e Desenvolvimento de Alternativas Energéticas – Universidade Federal do Pará, Belém (Brazil)

Abstract

Microgrid prosumers with distributed energy resources (DER) can participate in coordinated control strategies that benefit microgrid operation, such as reducing peak demand and improving PV hosting capacity. Recent literature presents several optimal DER management strategies considering methodologies usually based on mathematical models and simulation. This work evaluates the practical operation of two off-the-shelf bidirectional PV-battery inverters with DER management capability under different operating scenarios, accessing important practical aspects that are often ignored in the development of simulation-based strategies for energy management purposes. Device-specific practical operation constraints are identified, and it is shown that some of them should be considered in control strategies as key parameters invariably present in DER operation. The practical evaluation shows that operation constraints based on battery voltage may reduce DER flexibility; instead, it is recommended that manufacturers consider batteries' state of charge.

Keywords: microgrid, distributed energy resources, energy management, demand response

1. Introduction

The adoption of smart microgrids in both off-grid electrification and grid-connected applications is recognized as an alternative in distribution level to improve system reliability, controllability, and economic and energy efficiency. A fundamental aspect of smart microgrids is the active operation of distributed energy resources (DER) that can participate in various control and management schemes, such as demand response, voltage regulation and peak shaving.

In specific microgrid scenarios, to ensure that DER operation contributes positively to the system, it is essential to actively control such resources in a coordinated manner, considering the several operating constraints at both DER and grid levels. For example, an inverter-based DER operation is constrained to its maximum power rating, while the distribution grid operation is constrained, among other factors, to a permissible voltage range. In this context, recent literature presents various strategies of DER management in microgrids, with scopes ranging from off-grid applications (Ramabhotla *et al*., 2014; Suresh *et al*., 2020) to large-scale urban area systems (Ross *et al*., 2018; Sen and Kumar, 2018), with most of these works presenting a theoretical modeling approach that is validated by software simulation.

In practice, when it comes to small-scale DER control, there are off-the-shelf solutions that can manage different sources and loads, as is the case of hybrid inverters for PV-battery systems. Such devices are usually embedded with a set of standard operation strategies, such as peak-shaving, power-voltage and power-frequency droop logic, and battery charging cycling. Furthermore, device-specific parameters can be customized for specific control and management strategies, receiving real-time or day-ahead commands from a third-party operator (e.g., microgrid operator). Such functionalities make the adoption of optimal control strategies possible, targeting microgrid operation cost reduction while ensuring compliance to local power quality normative.

In this context, simulation-based theoretical approaches for optimal DER management strategies must consider the practical constraints that real systems and devices are subject to. Simple and practical models are always desirable as they make the development of optimal control at reduced computational cost possible. However, to make its practical implementation feasible, some constraints cannot be ignored, which inevitably add complexity to the model

Selection and/or peer review under responsibility of Scientific Committee
doi:10.18086/swc.2021.20.01 Available at http://proceedings.ises.org

and simulation process. Therefore, some simplified methodologies, though easy to implement, may have limited practical applicability.

This paper investigates key parameters that are often ignored in optimal DER energy management methodologies in smart microgrid applications. A lab-scale setup with multiple autonomous renewable energy systems is used to carry out the experimental tests (Manito *et al*., 2017). A detailed operational evaluation of off-the-shelf smart hybrid inverters from two different manufacturers is used to identify practical operational constraints that must be considered in optimal energy management strategies, thus providing valuable perceptions for the research community in the field.

2. DER test setup description

The DER setup that was used to carry out the experiments is located in the PV Systems Laboratory, part of the Institute of Energy and Environment of the Universidade de São Paulo. The experimental microgrid structure comprises four prosumers with energy management capability, two three-phase (ST1 and ST2) and two single-phase (SM1 and SM2) systems. Each prosumer has local PV generation and battery storage, and measurement devices are also installed at the point of connection with the microgrid. Tab. 1 specifies the DER of each prosumer.

Tab. 1: Prosumer specifications.

Prosumer	PV (kWp)	Storage (kWh)	Inverter (kW)	Prosumer	PV (kWp)	Storage (kWh)	Inverter (kW)
ST1	6.71	23.5	15	SM1	1.75	10.5	5.0
ST2	2.8	19.2	18	SM2	1.25	10.5	4.5

The microgrid setup can be configured to operate in two topologies, parallel and cascaded, and be connected to two different external sources (the utility grid and a diesel genset), making it possible to evaluate different management schemes. In the parallel configuration, all prosumers are connected to a common bus bar, as shown in Fig. 1(a). In the cascaded configuration, the prosumer ST1 is connected to the main supply, and the other prosumers are seen as local loads by the ST1 system (Fig. 1(b)). The cascaded configuration makes it possible to control the voltage and frequency at the point of common coupling between the prosumers, where ST1 operates as a microgrid forming system, interfacing the microgrid with the aforementioned external sources, and the other systems are microgrid's prosumers. An industrial real-time controller (RTC), from National Instruments's CompactRIO series, is responsible for setting the topology, monitoring and controlling the operation and several parameters associated with each controllable DER (*e.g.*, current dispatch setpoints). Meters are connected at the ac-side of each inverter.

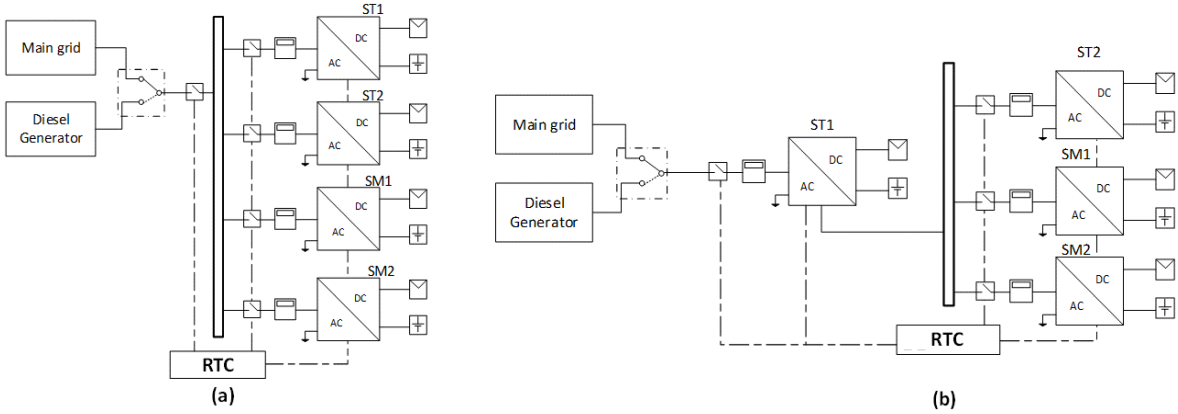

Fig. 1: Possible DER test configurations: (a) Parallel topology and (b) Cascaded topology.

The real-time controller, referred to as the Microgrid Central Controller (MGCC), hosts a Labview-based application that was developed considering the specific communication protocols associated with each inverter and its respective available monitoring and control variables. Therefore, a customized application was needed for each DER, increasing MGCC complexity and concept-to-implementation time. It is important to point out that the firmware of the tested off-the-shelf inverters was developed without compliance with DER interoperability standards, such as IEC 61850-7-420 (IEC, 2009), IEEE P2030.5 (IEEE, 2018) and SunSpec series of standards (SunSpec, 2021). The adoption of interoperability standards is key for developing scalable microgrid controllers and the adoption of practical DER

management strategies. The commercial inverters tested in this work were originally developed for off-grid electrification applications, but their main energy management functionalities related to grid-connected operation are present in their firmware, which enabled to test them in the microgrid setup depicted in Fig. 1. It is important to note that new devices developed specifically for grid-connected operation may comply with interoperability standards and are more oriented to smart energy management operation. Nonetheless, the practical considerations described in the following section hold true for the broader range of smart bidirectional inverters regarding the adequacy to simulation-based optimal energy management methodologies.

3. Real-time Tests and Results

To evaluate the real-time operation of the DER under MGCC commands and investigate the system's capacity to contribute to energy management strategies, two sets of tests were performed for a three-phase prosumer (ST2) and a single-phase prosumer (SM2), both operating in the microgrid cascaded topology. The tests were performed by the real-time adjustment of the inverter's parameters and prosumer's loads to emulate different operation conditions. The detailed procedure for each set of tests is described in the following items. The tested setpoints, such as charge and discharge current adjustments, were selected considering a set of different possibilities of energy management strategies that the devices could be submitted to in real-time or scheduled operation. The tests cover important operation modes in DER management, such as load peak shaving, grid feeding, and battery charging.

3.1. ST2 - Adjust battery charge and discharge setpoints

System ST2 is a three-phase system formed by the master-slave association of three 6 kW single-phase bidirectional inverters that share a DC bus bar rated at 48 V. It is not possible to directly control system ST2 power dispatch. Instead, the rms current must be adjusted using the parameters *max grid feeding current*, to determine the maximum current injection into the grid, and *maximum current of AC source*, that limits the current demanded from the external source. Furthermore, parameters *grid feeding allowed* and *charger allowed* are used to determine whether the system operates injecting or demanding current from the grid. Grid feeding current is constrained by parameters on both AC and DC sides. On the AC grid side, grid feeding current is limited by an increase in system frequency and voltage; on the DC side, battery voltage reduction also limits the grid feeding current parameter.

To exemplify the practical constraints associated with ST2 operation, the test results shown in Fig. 2 present the controlled dispatch by adjusting *max grid feeding current* and *maximum current of AC source* parameters, given different set points of current in both directions: microgrid-to-prosumer (positive active power) and prosumer-to-microgrid (negative active power). The test started with the battery fully charged. ST1 was disconnected from the main grid and was forming the microgrid's main AC bus bar.

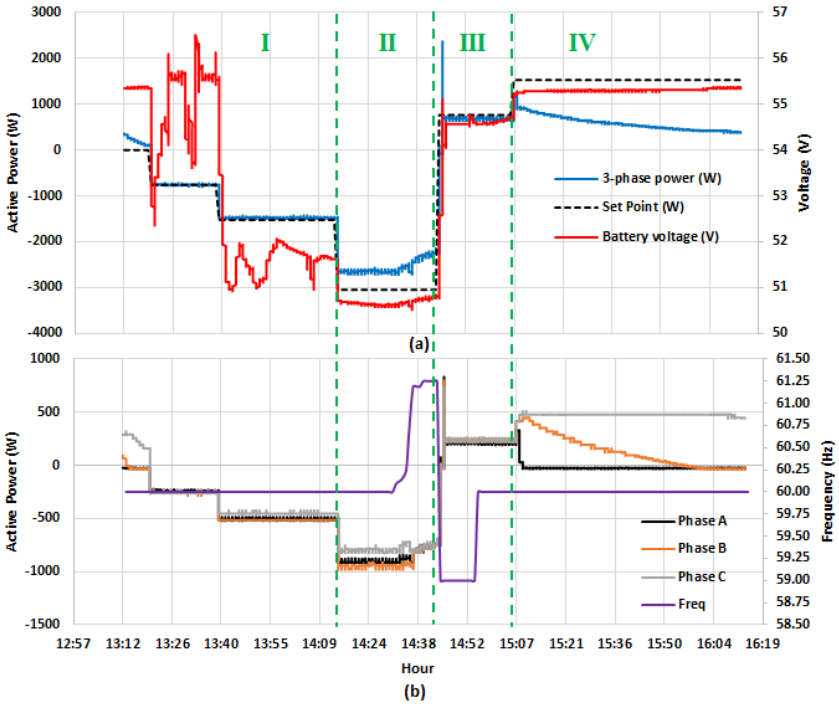

Fig. 2: ST2 charge and discharge test.

In the first half of the test (regions I and II), the ST2 battery bank was discharging, injecting power into the microgrid. As the injected power increases, battery voltage drops from 55.5 V to 50.8 V in approximately 1 hour, and the last discharge setpoint, in region II, was not achieved due to battery low-voltage constraint – even though the battery state of charge was within the admissible range. Furthermore, it is observed that at the end of region II, microgrid frequency increases as a result of P-f droop control of ST1, which further reduces the power injection from ST2. In the second half of the test (regions III and IV), ST2 demanded power from the microgrid to charge the battery bank. However, the demand setpoint in region IV (1.5 kW) was not reached as the high state of charge of the battery limited the charging power. Furthermore, during the power limiting event, unbalance was observed between the three phases of the system – which is a device-specific function to improve charging efficiency.

It is important to note that the battery bank used in the test presented in Fig. 2 was at the end of its service life (low state of health), and even small variations in charge or discharge current originate large variations on the battery voltage. This is clear in Fig. 2 region I, where the voltage variation is also associated to variations in the local PV generator output current.

3.2. SM2 – Peak Shaving and Microgrid Feeding

System SM2 is a single-phase system formed by a bidirectional converter rated at 4.5 kW, connected to a 48 V battery bank. As in ST2, it is not possible to directly control its power dispatch, being the rms current the variable that can be controlled by adjusting the parameters *Load Shaving Amps* and *Maximum Sell Amps*. These parameters determine the maximum current to be demanded from the grid and the maximum current to be fed into the grid, respectively. Furthermore, parameters *Grid Support*, *Charger Enable/Disable* and *Sell Enable/Disable* must be set according to the desired operation. SM2's inverter operation is very sensitive to battery voltage, as indicated in Fig. 3(a).

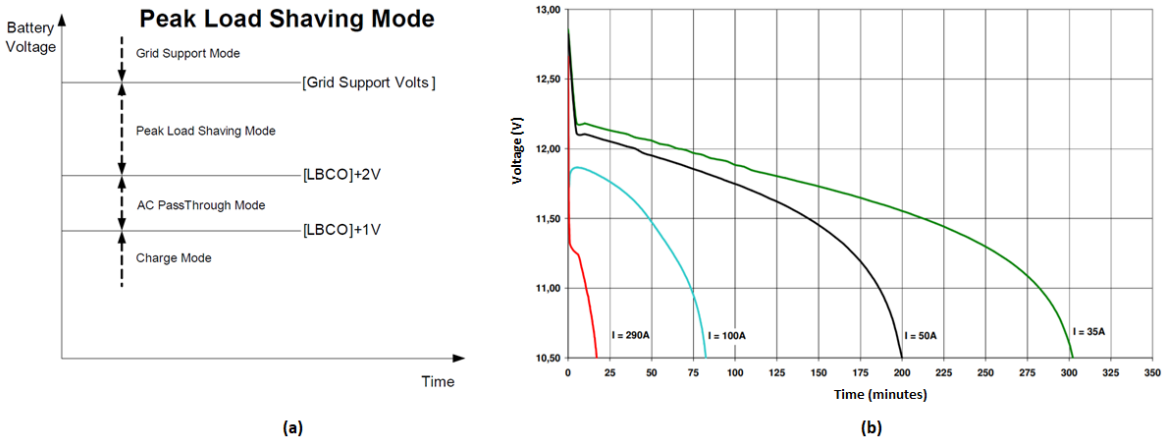

Fig. 3: (a) Converter operation modes as a function of battery voltage. Source: Schneider (2012). (b) 12 V Lead-acid battery typical discharge curves. Source Freedom (2008).

According to the inverter's manual, if the battery voltage is above the level defined by the parameter *Grid Support Volts* the inverter is capable of operating in grid support mode, which is to provide P-f, P-V and Q-V droop curves. When the battery voltage is below that level and above the level defined by the parameter *LBCO (Low Battery Cutout)* + 2V, the inverter can operate in peak load shaving (or grid feeding) mode, with maximum grid current set by *Load Shaving Amps*, as defined before. AC PassThrough Mode, shown in Fig. 3(a), bypasses the inverter and directly connects the local loads to the grid. In Charge Mode, the bidirectional converter operates as a rectifier to charge the battery, being a load to the system. Given this sensitivity to battery voltage, it is fundamental to properly determine the parameters within brackets in Fig. 3(a) to ensure that the inverter can operate according to an optimal dispatch strategy. A restricted set of parameters may reduce operational flexibility, while a broader range may reduce battery lifetime.

However, to optimally determine those parameters is not a simple task, as the battery voltage is highly dependent not only on its state of charge but also on the discharge current. An example of this dependence is shown in Fig. 3(b) for the 12 V lead-acid battery used to form SM2's battery bank.

To exemplify the practical constraints associated to SM2 operation, two tests were performed: peak shaving and microgrid feeding. Fig. 4 presents the results for the peak shaving test for different maximum microgrid current setpoints and local SM2 load. The purple dashed line indicates the maximum microgrid current setpoint, while the

solid green line indicates the current measured at the microgrid connection point, where positive values indicate microgrid-to-SM2 power flow. It can be seen that the inverter does not follow the maximum microgrid current setpoint. Most of the time, the actual measured microgrid current is above the *Load Shave Amps* level, even though battery current responds to changes in the peak shaving parametrization, as shown in Fig. 4(b).

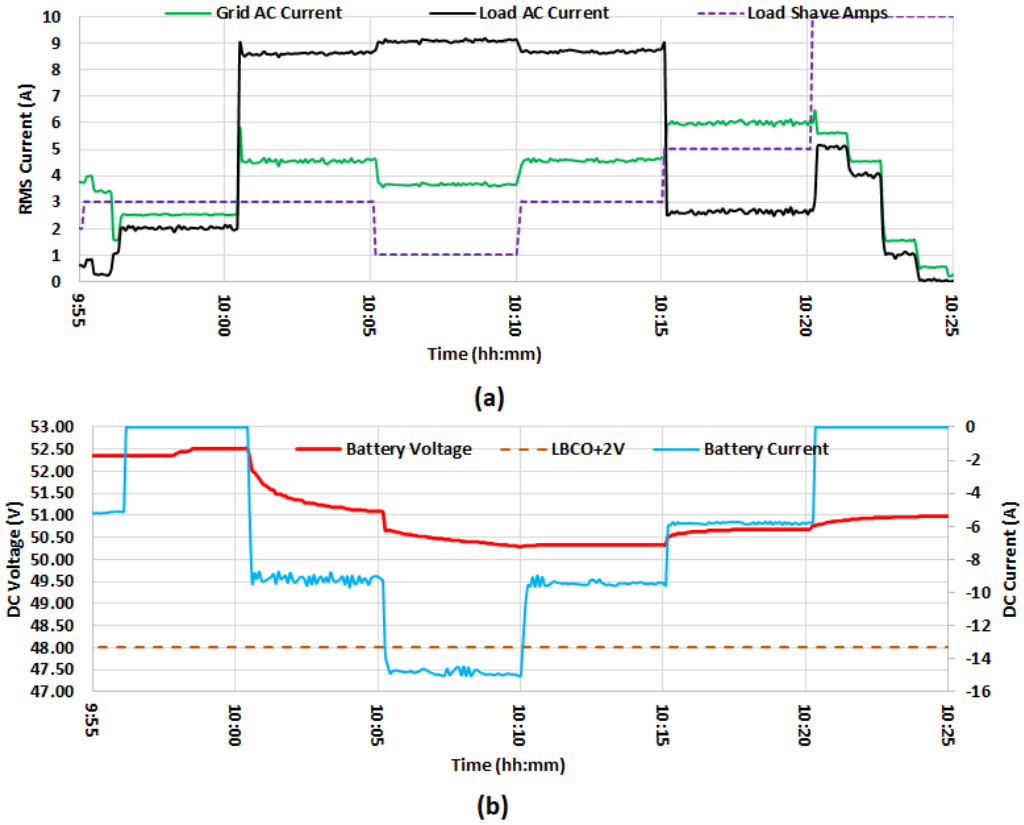

Fig. 4: SM2 peak shaving test. (a) AC load and grid current and (b) battery voltage and current.

Fig. 5 presents the test results for SM2 microgrid feeding operation. The red dashed line indicates the maximum microgrid feeding current setpoint, while the solid green line indicates the actual measured current at the microgrid connection point, where positive values indicate SM2-to-microgrid power flow. Fig. 5(a) shows that the device follows the microgrid feeding setpoint until 11h05, with a small error for low current levels. At 11h05, a step-change in the microgrid feeding setpoint from 5 A to 10 A triggers the AC side protection in the inverter, which changes from microgrid feeding mode to AC PassThrough mode, bypassing the inverter stage and directing the local loads supply to the AC input. The high frequency and voltage variation in the AC side, shown in Fig. 6, can explain the inverter disconnection. As the microgrid is formed by a static power converter (ST1), the AC coupling at SM2 is more susceptible to frequency and voltage variations during transients, as is the case of the abrupt change in the grid feeding setpoint.

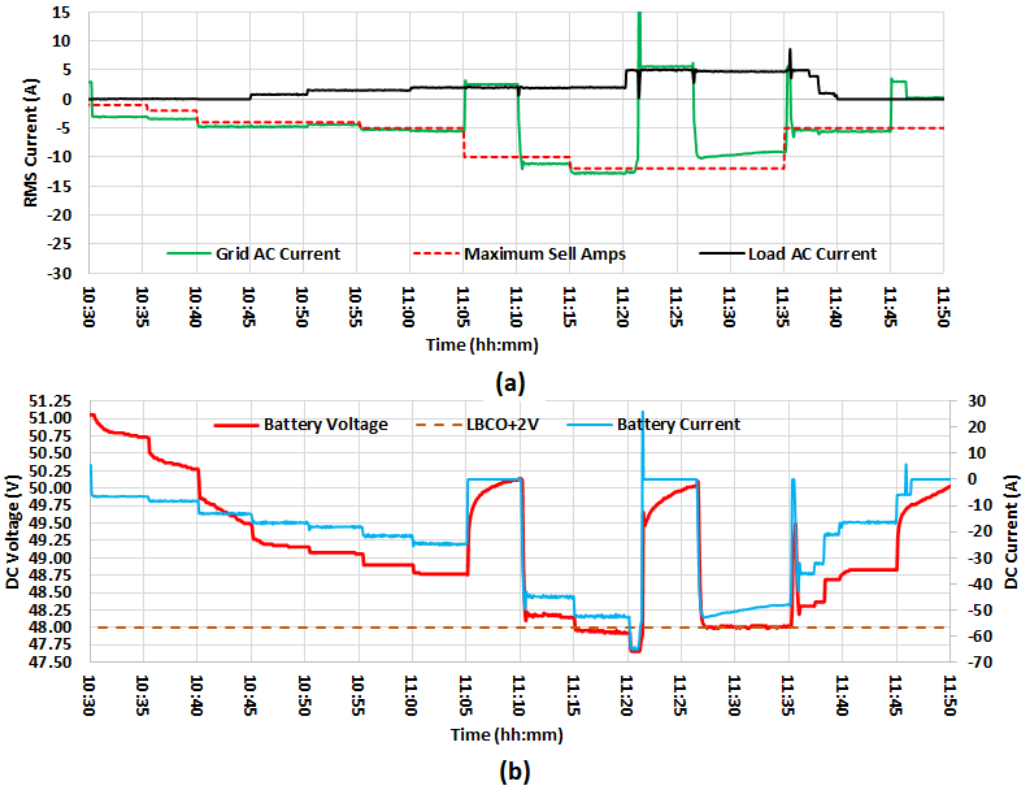

Fig. 5: SM2 grid feeding test. (a) AC load and grid current and (b) battery voltage and current.

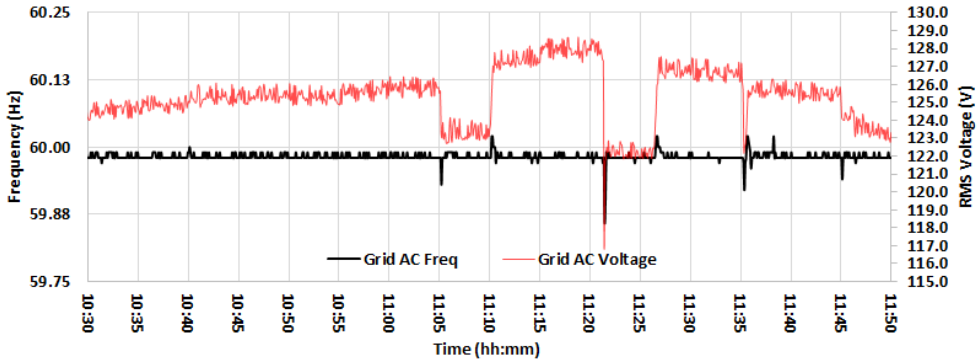

Fig. 6: Microgrid voltage and frequency during SM2 grid feeding test.

Fig 5(a) also shows that after five minutes the inverter reconnects and resumes microgrid-feeding operation (11h10), following the current setpoints with a small error. However, at 11h21, the inverter protection trips again, changing the operation from microgrid feeding to AC PassThrough. This time the tripping was caused by low battery voltage after a local load increase event at 11h20. In this test, the *LBCO* parameter was set to 46 V; therefore, battery voltages below 48 V (*LBCO* + 2V) disable grid feeding operation mode. Just like in the previous tripping, after a 5-minutes interval, the inverter resumes grid feeding operation as battery voltage increases, but at this time, the grid feeding current was limited to maintain the minimal allowable battery voltage level for this operation mode (48 V), thus not following the controller setpoint. As local loads reduce and controller grid feeding setpoint is set to 5 A (11h35), grid feeding operation resumes properly until a grid feeding disable command is given by the central controller at 11h45.

4. Conclusions

The experimental evaluation presented in this paper shows that energy management capable devices, particularly bidirectional PV-battery based converters, are subject to several operation constraints that highly affect system capacity to respond to an external energy management dispatch control. Furthermore, it is shown how specific parameters affect system operation for the different inverters to achieve similar tasks, highlighting the importance of interoperability standards to promote the development of scalable, plug-and-play energy management controllers.

The ST2 test presented two important operational characteristics that may affect system performance in terms of optimal dispatch and power quality. First, dispatch constraints due to battery voltage (*i.e.*, methodologies that use battery's state-of-charge as constraint are not adequate to be applied in this specific device) and second, three-phase unbalance during power limitation in battery rectifier operation (*i.e.*, single-phase equivalent) might not be adequate to evaluate the performance of this type of system.

The SM2 peak shaving test indicates that even though this system can follow setpoint commands from the central controller, it presents an offset error that could be corrected by implementing a feedback logic in the microgrid controller. On the other hand, SM2 responds accurately to grid feeding commands as long as the operational constraints are observed. In this respect, the need to set specific battery voltage-related parameters adds complexity to the central controller parametrization, as knowledge of battery characteristics is required to determine an optimal set of parameters. In this context, if this device used the battery state of charge as a control variable, the central controller implementation could be simplified and promote scalability to different energy storage characteristics.

Even though the tests focused on steady-state system operation given real-time changes in parameters and loads, it is also important to note the dynamic implications associated with the microgrid operation when formed by a static battery-based power converter with power rating close to the DER ratings in the microgrid. During the SM2 grid feeding test, abrupt grid feeding current setpoint changes originated AC-side voltage and frequency transients that tripped DER protection. Therefore, in this system, it is good practice for the microgrid central controller to prioritize smooth changes in operation setpoints whenever possible.

It is important to notice that the practical evaluations in this work were obtained for specific devices and operating conditions; therefore, it is not possible to generalize the results for a broader range of systems. Nonetheless, the tests provide useful perceptions of general DER characteristics that can affect system performance and must be observed when developing energy management applications with third-party central control, especially in the case of microgrids with high penetration of static converter devices. Further work will be developed considering daily system operation, to access the impact of controller parametrization and DER constraints on both energy and operation costs for the microgrid.

To summarize, the practical operation insights identified in this work are as follows:

- The microgrid controller logic must comply with the DER control logic when it comes to energy storage constraints, specifically whether the DER device considers the SoC or voltage as main constrain variables;
- When developing a microgrid model, there are cases in which it may be important to consider full three-phase models, as single-phase equivalents may not be adequate if three-phase DER devices operate unbalanced;
- When the microgrid-forming device is a static power converter with power ratings close to the ratings of the DER devices, dynamic constraints might affect the DER performances, such as ramp up or ramp down rates for power setpoint changes.

5. Acknowledgments

The authors would like to acknowledge Brazilian funding agency *CAPES – Coordenação de Aperfeiçoamento de Pessoal de Nível Superior* for the financial support (process n. 88887.609816/2021-00).

6. References

Freedom. Manual Técnico Bateria Estacionária série DF. 2008.

IEC. Communication networks and systems for power utility automation - Part 7-420: Basic communication structure - Distributed energy resources logical nodes. International Standard, 2009.

IEEE. P2030.5 - Standard for Smart Energy Profile Protocol. June 2018.

Manito, A., Novaes, K., Mocelin, A., Melendez, T., Pinho, J., Zilles, R., 2017. Integration of autonomous renewable energy generation systems with different topologies in a smart grid cluster to enhance performance in usual operational situations. Proceedings of the ISES Solar World Congress 2017. DOI:10.18086/swc.2017.03.01 Available at http://proceedings.ises.org.

Ramabhotla, S., Bayne, S., Giesselmann, M., 2014. Economic Dispatch Optimization of Microgrid in Islanded Mode.

Proceedings of the International Energy and Sustainability Conference 2014. Farmingdale, NY, USA. DOI: 10.1109/IESC.2014.7061838.

Ross, M., Abbey, C., Bouffard, F., Joós, G., 2018. Microgrid Economic Dispatch with Energy Storage Systems. IEEE Trans. Smart Grid, v. 9, i. 4, pp. 3039-3047. DOI: 10.1109/TSG.2016.2624756.

Schneider Electric. Xantrex XW Series Hybrid Inverter/Charger – Operation Guide. Doc. 975-0240-01-01, August 2012 Revision D.

Sen, S., Kumar, V., 2018. Microgrid control: A comprehensive survey. Annual Reviews in Control, v. 45, pp. 118-151. DOI: 10.1016/j.arcontrol.2018.04.012.

Studer Innotec SA. Xtender – User Manual. Studer Innotec SA 2015 – V 4.6.0.

SunSpec. SunSpec Modbus package, 2021. Available in: https://sunspec.org/specifications/. URL accessed on October 8th 2021.

Suresh, V., Muralidhar, M., Kiranmayi, R., 2020. Modelling and optimization of an off-grid hybrid renewable energy system for electrification in rural areas. Energy Reports, v. 6, pp. 594-604. DOI: 10.1016/j.egyr.2020.01.013.